Pulsar Scintillation Arcs reveal filaments in the Interstellar Plasma

Barney Rickett, Dan Stinebring, Bill Coles, and Gao JianJian

Citation: AIP Conf. Proc. **1357**, 97 (2011); doi: 10.1063/1.3615088
View online: http://dx.doi.org/10.1063/1.3615088
View Table of Contents: http://proceedings.aip.org/dbt/dbt.jsp?KEY=APCPCS&Volume=1357&Issue=1
Published by the American Institute of Physics.

Pulsar Scintillation Arcs reveal filaments in the Interstellar Plasma

Barney Rickett*, Dan Stinebring†, Bill Coles* and Gao, Jian-Jian*

*ECE Dept, UC San Diego, La Jolla, CA 92093-0407
†Physics Dept., Oberlin College, Oberlin, OH 44074

Abstract. Both forward and reverse Scintillation Arcs are seen in observations of several pulsars. We study the arcs, which are seen in the 2-D Fourier transform of the dynamic spectrum, from PSRs B0834+06 and B1737+13. In both cases we conclude that the underlying scattered image is highly extended along an axis and also highly modulated along that axis. The corresponding spatial structure in the ionized interstellar medium must be bundles of spaghetti-like filaments – highly anisotropic turbulence (on scales of 1000-10000 km) which is also very intermittent on scales of an AU. We speculate on their possible origin as remnant turbulence from long past supernovae.

Keywords: Pulsar, Scattering, turbulence, interstellar plasma
PACS: 98.38.-j, 52.35.Ra, 95.30.Qd, 41.20.Jb

Interstellar Scintillation Arcs

As pulsar observers know well, interstellar scintillation (ISS) causes deep fluctuations in the dynamic spectrum of pulsar radio pulses over typical times of a minute and bandwidths of 10 kHz. Such fluctuations also broaden the pulse and cause its arrival time to vary. Although this is a nuisance for understanding the pulsar or searching for gravitational waves, it provides an important probe of fine structure in the ionized interstellar medium (IISM) [7]. In studies of ISS over four decades the IISM is often modelled by homogeneous turbulence in the electron density with an isotropic Kolmogorov spectrum versus wavenumber.

An entirely new view of the phenomenon is provided by the discovery of scintillation arcs by Stinebring et al. [8]. The dynamic spectrum of ISS often has bright features that drift in frequency over minutes and sometimes drifts are visible in both directions creating a criss-cross pattern. The arc phenomenon is revealed by plotting the 2-D Fourier power spectrum of the dynamic spectrum. This is called the secondary spectrum versus transform variables: differential delay $\tau(\mu\text{sec})$ and differential Doppler frequency f_D (mHz). Stinebring et al. [8] showed that the main feature in the secondary spectrum of many pulsars is concentrated near a parabola ($\tau \propto f_D^2$). In some cases this "arc" is broad and fuzzy and in others it is sharply defined and there are many variations between these extremes.

The specific example of PSR B0834+06, shown in the left panel of Figure 1, was published by Hill et al. [4]. Power is concentrated in a forward arc near the dashed parabola but consist of small reversed "arclets" whose apexes lie near the parabola and have the same (reversed) curvature. The basic forward parabola can be explained by the interference between two waves, one with no scattering and the other scattered at angles

Radio Pulsars: An Astrophysical Key to Unlock the Secrets of the Universe
AIP Conf. Proc. 1357, 97-100 (2011); doi: 10.1063/1.3615088

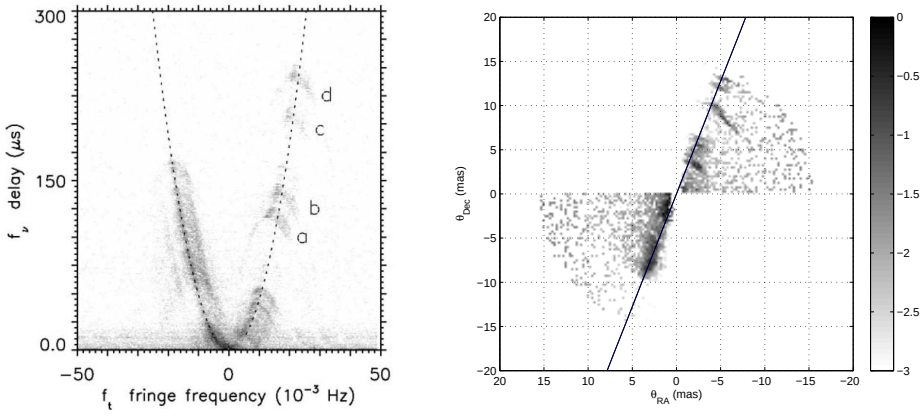

FIGURE 1. *Left:* The secondary spectrum of PSR B0834+06 recorded near 327 MHz at Arecibo in January 2004 [4]; the darkness of the grayscale is logarithmic in power and covers a total range of $\sim 10^5$. The primary forward arc follows the parabola shown by a dashed line. Note the the four isolated reversed arclets labeled a,b,c,d. *Right* : Scattered image estimated from scattered electric field components obtained by Walker et al., (2008) for the same pulsar from the same sequence of ISS observations as that in the left panel. The scattered brightness is plotted versus offsets (in milliarcseconds) from the RA and Dec of the pulsar. Color bar gives $\log_{10}$ of brightness. The inversion, which relies on the vector proper motion of the pulsar [6] and the DM distance (643 pc), suffers from a two-fold ambiguity. The image is plotted after the ambiguity is resolved by flipping the upper quadrant about the velocity direction, based on our VLBI astrometry [1]. The major axis from the astrometry is shown by the blue line. The reverse arclets b,c & d appear as three bright groups of pixels in the upper right, which lie near the blue line, while a is displaced to the right of b.

$\sim$ milli-arseconds (see the theory in Stinebring et al. [8], Cordes et al. [2], Walker et al. [9]). The Doppler frequency axis maps into the difference in angle (projected along the direction of transverse motion) and the delay axis maps to the difference in the *squares* of the two angles of deflection. Thus the secondary spectrum maps the scattered image (brightness distribution caused by interstellar scattering) through a quadratic coordinate transformation.

The reverse arclets are due to isolated points of high brightness interfering with an extended central peak in brightness; the fact that the interiors of the parabolae are empty can only be explained if the central region in brightness is very anisotropic. The arclets labelled a-d are notable and were seen to move systematically to larger delays over the 20 day sequence of observations. The rate of their movement was found to be in close agreement with that due to the proper motion of the pulsar. In other words the sites of the scattering appeared to remain fixed in the IISM as the pulsar swept by. The existence of such localized scattering suggests very intermittent turbulence in the IISM.

Anisotropic Scattering: PSR B0834+06 & B1737+13

In more recent observations of the same pulsar Brisken et al. [1] observed its ISS with 4 large antennas over trans-Atlantic baselines. The data were analyzed with very high spectral resolution using the software correlator at Swinburne. Using a novel secondary

spectrum analysis of the visibility on each baseline we were able to map the angular positions of the scattered waves responsible for the discrete reverse arclets, which were similar to those in Figure 1 although they differed in detail. The results showed the peaks of the scattering to be spread out along a straight line inclined at about 25 degrees to the declination axis. This confirms that the scattered image is very anisotropic, but since the astrometric technique does not give the brightness we could not estimate its axial ratio.

The data of Hill et al. [4] were further analyzed by Walker et al. [10] who modeled the received radiation as a summation of 8000 complex scattered electric field components. We have found that their amplitudes, which are given as a function of Doppler frequency and delay, can be transformed to estimate the 2-D scattered brightness. The right panel of Figure 1 shows the image to be highly elongated along an axis, which agrees closely with that found by Brisken et al. [1] whose observations were 21 months later. One can infer an effective axial ratio of 10:1 or more from the ratio of the widths of the features parallel and perpendicular to the axis.

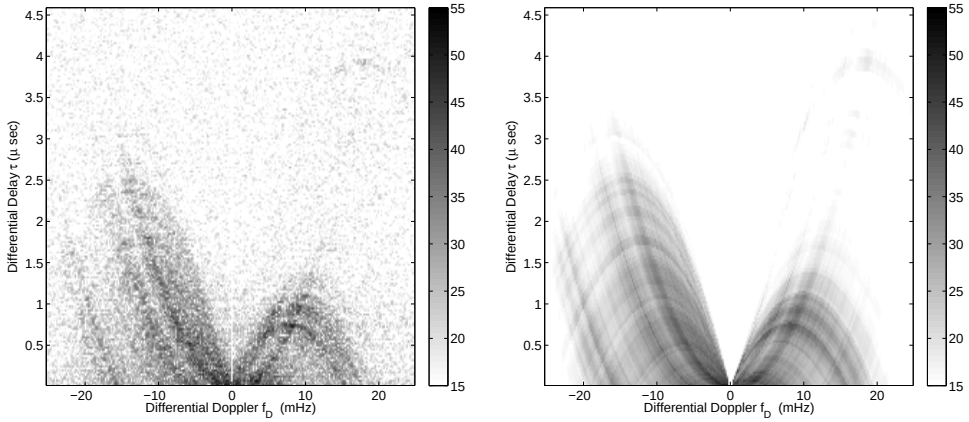

FIGURE 2. *Left:* The secondary spectrum of PSR B1737+13 recorded near 1425 MHz at Arecibo on MJD 53857. *Right* : 1-D scattering model fitted to data on left. The tablets (colour on-line) are in dB.

We have also investigated the arcs in 36 weekly ISS observations of PSR B1737+13 reported by Hemberger & Stinebring [3]. They emphasized the pronounced variation in the secondary spectra and its influence on pulsar arrival times. Here we analyze the reverse arclets in the secondary spectra which predominated during the first 10 weeks. The left hand panel of Figure 2 shows arcs in the secondary spectrum in May 2006. Since the spectra are reflection symmetric about the origin, the prominent reverse arc with an apex near 9 mHz intersects Doppler axis near 15 mHz and its reflection re-appears at –15 mHz as a sloping feature extending to 1μsec in delay.

Consider a 1-D model in which the scattered brightness varies as $B(\theta_p)$ along some axis and is infinitessimally thin in the orthogonal direction. As shown by Cordes et al. [2] the secondary spectrum at τ, f_D is then $\propto B(\tau/Af_D + Af_D) \times B(\tau/Af_D - Af_D)/|f_D|$. We fitted this model to the observed secondary spectrum by optimizing the curvature parameter A and 200 values of $B(\theta_p)$. As can be seen the model provides a very good fit to the arc features both in amplitude and location. We conclude that for this pulsar too the scattering is highly anisotropic. In order to estimate the axial ratio we are extending the model to 2-D. The perpendicular width is most sensitively estimated near the origin where the secondary spectrum exhibits a V-shaped notch.

Interstellar Plasma Filaments

The angles of deflection that cause the arclet behavior can be used to constrain the local electron density n_e. For PSR B0834+06 we find $n_e \gtrsim 10$ cm^{-3}. Such high densities are far from pressure balance and with the high degree of anisotropy they imply the influence of strong magnetic fields. The spatial structure in the plasma can only be inferred indirectly from the scattered image. The first interpretation is that spatial structures are filamentary aligned by the magnetic field perpendicular to the axis of angular scattering. The density of the filaments must also vary perpendicular to the magnetic field to account for the discrete nature of the arclets. This could be described as bundles of spaghetti-like filaments. Alternative geometrical interpretations are possible with sheets instead of filaments or with isotropic turbulence that is only present in elongated regions parallel to the scattering axis (see Brisken et al. [1]).

Although the Hα maps show no signs of structure toward PSR B0834+06, we speculate that filaments originate from turbulence generated in a long past supernova shell. One can estimate that expanding supernovae shells cross any given point in the Galaxy every few million years. Thus bursts of anisotropic turbulent plasma could travel through the IISM and leave fossil (i.e. decaying) turbulence that causes the arcs. This idea is highly speculative since the scales visible in young supernova remnants are more than 5 orders of magnitude larger than those in the image of Figure 1. Further it requires that turbulence on AU scales occasionally survives for as long as a million years, which is two orders of magnitude longer than predicted recombination time for 10 cm^{-3} enhancements in plasma density.

An important consequence of this work for pulsar timing is that intermittence in the properties of the IISM may cause greater variations in arrival times than would be predicted from the standard assumption of uniform isotropic Kolmogorov turbulence.

Acknowledgements. We thank Mark Walker for sharing his analysis of Dan's data; Coles & Rickett thank the NSF for partial support under grant AST 0507713. We thank Jocelyn Bell for her discovery that has so greatly enriched astrophysics.

REFERENCES

1. W. F. Brisken, J.-P. Macquart, J. J. Gao, B. J. Rickett, W. A. Coles, A. T. Deller, S. J. Tingay, C. J. West, *Ap.J.*, **708**, 232–243, (2010).
2. J. M. Cordes, B. J. Rickett, D. R. Stinebring, & W. A. Coles, *Ap.J.*, **637**, 346–365 (2006).
3. D. A, Hemberger and, D. R. Stinebring, *Ap.J.*, **674**, L37–40 (2008).
4. A. S. Hill, D. R. Stinebring, C. T. Asplund, D. E. Berwick, W. B. Everett and N. R. Hinkel, *Ap.J.*, **619**, L171–174 (2005).
5. A. S. Hill, R. A. Benjamin, G. Kowal, R. J. Reynolds, L. M. Haffner and A. Lazarian, *Ap.J.*, **686**, 363-378, (2008).
6. A. G. Lyne, B. Anderson, & C. J. Salter, *MNRAS*, **201**, 503–520, (1982).
7. B. J. Rickett, *Ann. Rev. Astron. Ap.* **28**, 561–605, (1990).
8. D. R. Stinebring, M. A. McLaughlin, J. M. Cordes, J. M. Becker, J. E. Espinoza Goodman, M. A. Kramer, J. L. Sheckard & C. T. Smith, *Ap.J.* **549**, L97–100, (2001).
9. M. A. Walker, D. B. Melrose, D. R. Stinebring, & C. M. Zhang, *MNRAS*, **354**, 43–54 (2004).
10. M. Walker, L. Koopmans, D. Stinebring, W. van Straten, *MNRAS*, **388**, 1214–1222 (2008)